Editors' Suggestion

Path-Dependent Supercooling of the ^{3}He Superfluid $A-B$ Transition

Dmytro Lotnyk,[1] Anna Eyal,[1,2] Nikolay Zhelev,[1] Abhilash Sebastian,[1,3] Yefan Tian,[1] Aldo Chavez,[1] Eric Smith,[1] John Saunders,[4] Erich Mueller,[1] and Jeevak Parpia[1,*]

[1]*Department of Physics, Cornell University, Ithaca, New York 14853, USA*
[2]*Physics Department, Technion, Haifa 3200003, Israel*
[3]*VTT Technical Research Centre of Finland Ltd, Espoo 02150, Finland*
[4]*Department of Physics, Royal Holloway University of London, Egham TW20 0EX, Surrey, United Kingdom*

(Received 6 January 2021; revised 22 March 2021; accepted 27 April 2021; published 25 May 2021)

We examine the discontinuous first-order superfluid ^{3}He A to B transition in the vicinity of the polycritical point (2.232 mK and 21.22 bar). We find path-dependent transitions: cooling at fixed pressure yields a well-defined transition line in the temperature-pressure plane, but this line can be reliably crossed by depressurizing at nearly constant temperature after transiting T_c at a higher pressure. This path dependence is not consistent with any of the standard B-phase nucleation mechanisms in the literature. This symmetry breaking transition is a potential simulator for first order transitions in the early Universe.

DOI: 10.1103/PhysRevLett.126.215301

Superfluid ^{3}He is a condensed matter system with a complex order parameter. Superfluidity onsets with the condensation of pairs into a state with finite angular momentum via a second order phase transition at a pressure dependent transition temperature, T_c [1–5]. Pressure dependent strong coupling favors the anisotropic A phase at high pressures, while the isotropic B phase is the stable phase below the $T_{AB}(P)$ line [6]. Under these conditions the equilibrium phase diagram exhibits a polycritical point (PCP) at which the line of first order transitions (T_{AB}) intersects the line of second order transitions (T_c) at 21.22 bar and 2.232 mK [Fig. 1(a)]. The transition between the A and B phases is first order and thus subject to hysteresis. At the PCP, the bulk free energies of A, B superfluid phases and normal state are equal.

At high pressure the A phase supercools well below T_{AB} and can be long lived [8]. A phase supercooling occurs because any formation of a bubble of radius r of the B phase (from the parent A phase) sets off the unusually large interfacial energy ($\propto r^2$) [9] against the small free energy gain ($\propto -r^3$) [10] leading to a critical radius ≈ 1 μm. The extreme purity and low temperatures that limit thermal fluctuations together with the barrier to homogeneous nucleation lead to calculated lifetimes of the supercooled A phase greater than the age of the Universe. The transition has been the subject of extensive experimental investigations [8,11–20] (summarized briefly in Supplemental Material Note 1 [21]) that have limited applicability to the results in this Letter since they were performed in a variety of magnetic fields and not focused on the PCP. The $A \rightarrow B$ transition was also the subject of extensive theoretical investigations [29,34–40]. As Leggett has pointed out [29,35,36], the nucleation mechanism of the B phase "remains a mystery." Its study represents a unique opportunity to gain fundamental insights and is potentially relevant to phase transitions in the evolution of the early Universe [41].

Here we study the nucleation of the B phase in a well characterized isolated volume and in negligible magnetic field (≤ 0.1 mT) near the PCP. In this region the free energy landscape as a function of complex order parameter, pressure and temperature is of particular interest. Over the limited P, T phase space [box in Fig. 1(a)] we observe both a reproducibility of B phase nucleation and an unexpected path dependence.

Two mechanisms for nucleation of the B phase have experimental support. The "baked-Alaska mechanism" [29] requires local heating by deposition of energy following passage of a cosmic ray or charged particle and was

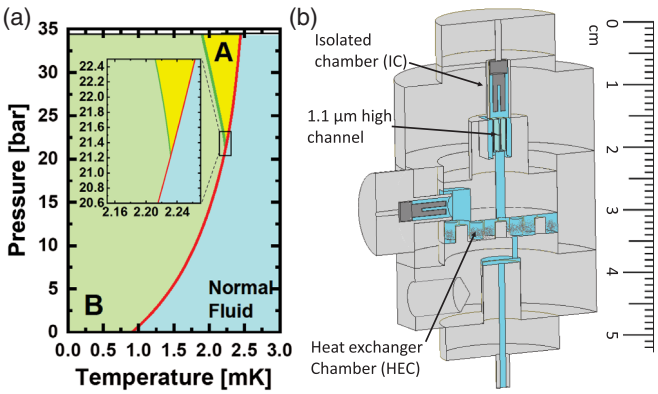

FIG. 1. (a) The phase diagram of ^{3}He [6,7], showing the extent of the equilibrium A phase (yellow), the B phase (green) separated by the equilibrium T_{AB} line (green). Superfluidity onsets at the T_c line (red). The region investigated here is within the box centered on the polycritical point. (b) Schematic of cell.

tested using quartz cells of roughness < 10 nm [8,42] in a magnetic field of 28.3 mT. The $A \rightarrow B$ transition could be induced by a nearby radioactive source, confirming aspects of the mechanism. In the cosmological or Kibble-Zurek scenario [19,37,38], small regions undergo phase transitions that are "oriented" differently under quench conditions (cooling through T_c) [17,19,43]. When they eventually coalesce, they produce a cosmic string, or its equivalent in ^{3}He—a vortex line. Other, yet to be tested models, cite Q balls [39] and resonant tunneling (RT) [40]. RT is an intrinsic nucleation mechanism, in which the transition rate into the equilibrium B phase (true vacuum) depends on the details of the order parameter landscape. Under certain precise conditions of temperature and pressure a nearby false vacuum facilitates the transition. Thus the mechanism relies on the richness of the superfluid ^{3}He 18-dimensional order parameter, with multiple possible states [44,45]. Furthermore some of these states have degeneracies, which are broken by weak interactions, for example, spin-orbit interaction. An example of this is the spatially modulated B phase, stabilized by confinement [46], which may explain the observed absence of supercooling in Ref. [47].

Our experiment consists of two chambers [Fig. 1(b)], filled with bulk ^{3}He separated by a $D = 1.1$ μm height channel. The experimental setup and the associated thermal parameters are described in detail in a previous publication [30] (see also Supplemental Material, Note 2 [21]). The $A \rightarrow B$ transition is observed in an isolated chamber (IC) using a quartz tuning fork [48] whose resonant frequency f and Q (quality factor, $Q = f/\Delta f$ with Δf the full linewidth at half power) are monitored continuously. The second chamber (HEC) contains the silver heat exchanger, as well as a second tuning fork. Nucleation of the B phase in the HEC does not propagate into the IC, because the A phase is stabilized in the channel by confinement [49] under all conditions studied here. There are no sintered powders in the IC to promote nucleation of the B phase but the surfaces are not specially prepared. The experiment is located where the magnetic field is ≤ 0.1 mT, the ^{3}He pressure, P was regulated to within the ± 0.01 bar using a room temperature gauge (see Supplemental Material, Note 3 [21]). Temperatures T were read off from a ^{3}He melting curve thermometer [6] after correction for thermal gradients (≤ 15 μK [30]) and converted to the PLTS2000 temperature scale [7] (Supplemental Material, Note 4 [21]). The temperature T (read off from the melting curve thermometer) and pressure P read off from a regulated pressure gauge located in the room temperature gas handling system accurately represent the T, P coordinates in the IC and HEC during all parts of the experiments (see Supplemental Material, Note 3 [21]).

The measured Q of the IC fork while cooling (blue) and warming (red) through T_c, and the $A \rightarrow B$ (blue) or $B \rightarrow A$ (red) transitions are shown in Fig. 2. The displacement of

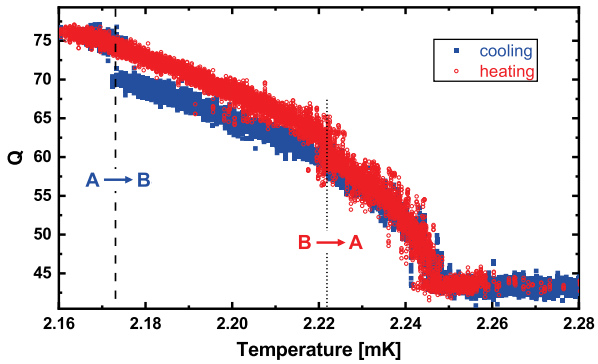

FIG. 2. The quality factor Q of the quartz fork in the isolated chamber while cooling (solid blue squares) and warming (open red circles) at 21.8 bar. Dashed lines mark the supercooled $A \rightarrow B$ and $B \rightarrow A$ transitions.

the dashed lines in Fig. 2 illustrates supercooling via the hysteresis of the first order $A \rightarrow B$ ($B \rightarrow A$) phase transitions. We cooled to within 5μK of the supercooled transition at 22 bar and maintained the temperature within 5μK of that transition for a day and observed no $A \rightarrow B$ transition, emphasizing the stability of the metastable A phase close to the observed supercooled transition temperature.

The P, T of the $A \rightarrow B$ supercooled phase transitions while ramping temperature at ≤ 10 μK/hr is shown in Fig. 3(a) as left-pointing triangles with a heavy blue line drawn to guide the eye. These points lie below the equilibrium T_{AB} line (light green) at zero magnetic field [6] where the free energies of the A and B phases are equal. The light green and heavy blue lines bound the supercooled A phase (light yellow). We observed the $A \rightarrow B$ transition at 20.89 bar ~ 24 μK below T_c but no $A \rightarrow B$ transition was seen at 20.88 bar (Supplemental Material, Note 5 [21]). Thus we do not extend the blue line to T_c; instead, we draw a gray dashed line at 20.88 bar. Clearly, the A phase is reliably observed while cooling at constant pressure through T_c below the polycritical point; however, it does not reappear on warming at these pressures. This confirms that the magnetic field, which would otherwise stabilize a thin sliver of the A phase, is negligible. The set of $A \rightarrow B$ transitions observed in the HEC along with the transitions shown here in the IC are briefly discussed in Supplemental Material, Note 5 [21]; the presence of silver powder significantly raises the temperature of $A \rightarrow B$ transitions.

To sample the $A \rightarrow B$ transition statistics, we increased the drive voltage to the quartz fork in the IC (by 10×) for a few hundred seconds, to warm the IC above T_c and then cool back through T_c and $T_{A \rightarrow B}$ as rapidly as possible (~ 100 μK/hr at $T_{A \rightarrow B}$). Warming the IC above T_c is essential to prevent premature nucleation by persistent pockets of B phase [20]. The Q following these pulses is shown in Figs. 3(b),3(c) (see also Supplemental Material, Note 5 [21]). The ^{3}He in the channel is certainly in the A

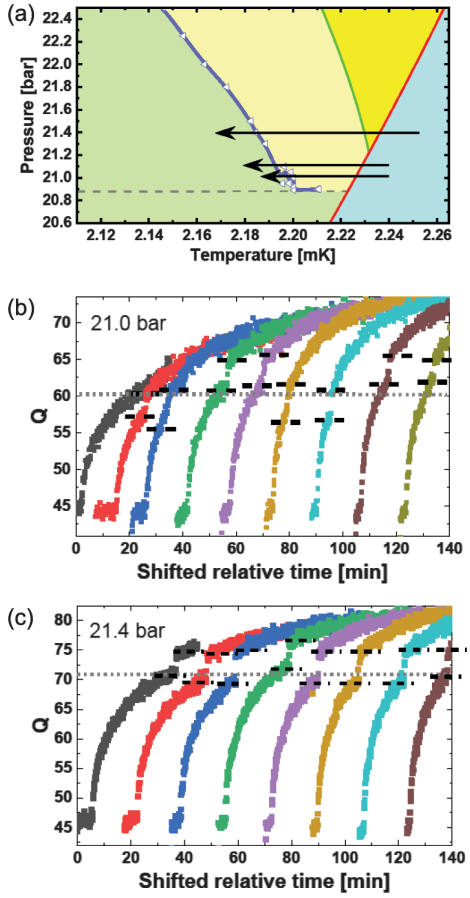

FIG. 3. (a) The red line marks the second-order phase transition $T_c(P)$, from the normal liquid (blue) to the superfluid state. The light green line $T_{AB}(P)$, marks the limit of the equilibrium A phase (dark yellow), where the $B \rightarrow A$ transition is seen on warming. Blue, left-pointing triangles and the heavy blue line (guide to the eye) bound the supercooled A phase (light yellow). The gray dashed line at 20.88 bar shows the limit of the supercooled A phase observed under slow constant pressure cooling at ≤ 10 μK/hr. A series of fast-cooled (~0.1 mK/hr) transitions ($Qvs..$ time) are shown at 21.0 (b) and 21.4 bar (c) following heat pulses that carry the IC into the normal state. The Q of slow supercooled transitions (see Fig. 2) are marked by dotted gray lines. In (a) the arrows show trajectories of fast and slow cooled transitions including at 21.1 bar. For the full set of low pressure fast and slow cooled transitions and discussion of the stability of the A phase below the PCP, see Supplemental Material, Notes 5–7 [21].

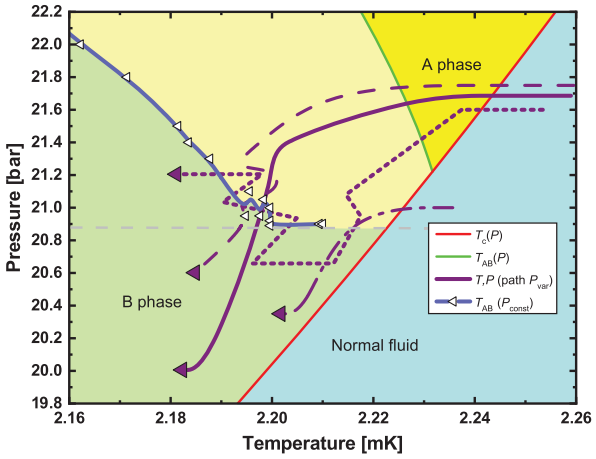

FIG. 4. The path shown in dotted purple crossed the constant pressure cooled supercooled transition line (heavy blue line) at several points. Solid, dashed, and dot-dashed purple lines depict paths followed, where cooling at constant pressure was followed by depressurization. $A \rightarrow B$ transitions are denoted by purple triangles.

phase before the IC cools through T_c [30,47,49,50] and the ^{3}He in the HEC is in the B phase. In Fig. 3(b), the $A \rightarrow B$ transition occurs in a very narrow interval of Q (and thus T). The width of the distribution of $T_{A\rightarrow B}$ at 21.4 bar is $\sigma = 3.6$ μK, close to the slow cooled $T_{A\rightarrow B}$, and similarly for 21.1 bar, $\sigma = 3.0$ μK. At 21.0 bar, the fast cooled $A \rightarrow B$ transitions were more broadly distributed ($\sigma = 6.0$ μK). The distributions are shown in Supplemental Material, Note 5 [21]. Pulsed experiments at 20.95 and 20.90 bar showed only a few $A \rightarrow B$ transitions with most pulsed transitions crossing directly from the normal to the B phase. Slow cooled $A \rightarrow B$ transitions were seen at 20.95, 20.92, 20.90, and 20.89 bar. These various slow and fast cooled transitions are shown in Supplemental Material, Note 5 [21]. The scatter in T_{AB} and increase in width of the distribution for fast cooled transitions at low pressures argues for the onset of an instability of the A phase under cooling at constant pressure from T_c. The initiation of the A phase while cooling at constant pressure through T_c below the PCP is briefly discussed in Supplemental Material, Note 6 [21]. Termination of this instability line away from T_c, similar to a critical point (see Ref. [21]), is not excluded.

Despite the sharpness of the (blue) instability line at constant pressure, we now show that nucleation of the B phase is path-dependent. We carried out a series of experiments where we followed different trajectories in the P, T plane (Fig. 4). It is clear that supercooling of A phase below the instability line (in one case involving several crossings of this line) is possible. Traversal of the gap between the apparent termination of the instability line and T_c is also possible. If the transition observed under constant pressure cooling were due to an enhanced transition probability at (or near) certain values of (P, T), then we should have observed an $A \rightarrow B$ transition on crossing the $T_{A\rightarrow B}$ ($P = $ Const.) line. We conclude that P, T are insufficient to describe the probability of the change of state of the system.

In another series of experiments we find an enhanced region of supercooling (striped region in Fig. 5) if we initially cool through T_c between 23 and 22 bar. This cooling is followed by a trajectory (paths not shown) in which we depressurize and cool slowly, all trajectories crossing the blue instability line below 21.5 bar. The

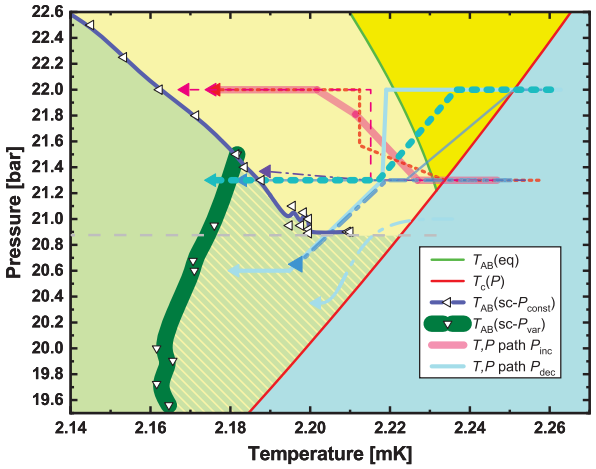

FIG. 5. Cyan lines, with differing symbols show paths from 22 to 21.3 bar, from 22 to 20.6 bar and from 21.3 to 20.6 bar, to observe $A \rightarrow B$ transitions (blue triangles). $A \rightarrow B$ transitions were also observed after cooling through T_c at 21.3 bar and then pressurizing to 22 bar (pink and purple lines with differing symbols), terminating in pink and purple triangles. $A \rightarrow B$ transitions observed following depressurization (or pressurization) retain memory of the pressure that T_c was traversed at since they supercool deeper (or less) than their constant pressure cooled counterparts. Supercooled $A \rightarrow B$ transitions (paths not shown) that crossed through T_c at pressures between 23 and 22 bar, and then cooled through the "blue line" below 21.5 bar, while depressurizing are shown as downward pointing triangles along a broad green line (guide to the eye).

supercooled $A \rightarrow B$ transitions occur along a reasonably well-defined line in the P, T plane shown as a broad green line in Fig. 5. This path-dependent enhancement of the supercooled region suggests a memory of T_c at which the normal-superfluid transition occurred. Such a memory or path dependence is confirmed since *undersupercooling* (albeit small) is seen after pressurization, (pink lines in Fig. 5); similarly, depressurization following cooling at a constant pressure results in *greater* supercooling (cyan lines in Fig. 5) compared to cooling at constant pressure through T_c to the same final pressure.

In summary, we have carried out a study of the nucleation of the superfluid B phase of ^{3}He from the supercooled A phase in the vicinity of the polycritical point, where the difference in free energy of the two phases is small. On cooling at *constant pressure*, we identify a well-defined instability line in the P, T plane at which the first order supercooled $A \rightarrow B$ transition occurs. We find that this instability line appears to terminate at a point, separated from the line of second order normal-superfluid transitions T_c, and at a pressure 0.3 bar below PCP. The locus of the instability line does not depend on the cooling rates studied, which differ by an order of magnitude, except in the immediate vicinity of the terminus point. However, by following a variety of different trajectories in the P, T plane we demonstrate that supercooling displays a path dependence. Thus pressure and temperature alone do not provide coordinates to specify where the supercooled A phase transforms to the B phase. An open question is the potential analog with path dependence in supercritical region of classical liquids [31], which may also relate to the observed terminus of the instability line.

We find that supercooling can be enhanced by crossing T_c and then depressurizing. In principle such a memory effect could be explained by small ^{3}He-filled cavities in the surface connected to the bulk ^{3}He via a narrow orifice (see Fig. 1 in [29]). However we believe this is not a likely mechanism here (see Supplemental Material, Note 8 [21]). Our experiment also provides a test of the baked-Alaska mechanism of cosmic ray induced nucleation in a well-motivated but relatively unexplored region of phase space near the PCP. We believe that neither the statistics of nucleation at the constant pressure instability line, nor the path dependence of nucleation are explained by this model.

We suggest that the full free energy landscape in the isolated chamber should be taken into consideration, within the framework of resonant tunneling or alternative models. The equilibrium order parameter has a strong spatial dependence: at surfaces of the chamber and the tuning fork, where gap suppression depends on surface scattering; at sharp corners [46,51,52]. The orientation of the order parameter (texture) in the complex geometry of the chamber and tuning fork may also play a role, although in this case the energy scales are much smaller [1,5]. Superfluid domain walls, both textural and cosmic [53] may also play a role [54] and respond differently under (de)pressurization. All these effects are in the context of the bulk free energy landscape of the superfluid ^{3}He order parameter, in which strong coupling effects (source of stability of A phase) are both pressure and temperature dependent [55].

Further investigations of these phenomena will be aided by the following. Surface scattering conditions can be tuned from diffuse to specular by adjustment of surface ^{4}He boundary layer [52,56,57]. The free energy difference of bulk A and B phases can be tuned by magnetic fields [32]. Surface quality and geometry can be tailored using silicon nanofabrication techniques [33,47,58], extending the method of confining channels adopted in this work to isolate the chamber from the B phase. The $A \rightarrow B$ transition can be assayed by a noninvasive probe, such as NMR [46,59]. It remains to be explored whether such path dependence is confined to the restricted region near the polycritical point.

We conjecture that the puzzling detachment of the constant pressure instability line and the reliable nucleation of the A phase below the PCP, may arise from the fact that the sample is cooled through a channel in which the A phase is stabilized by confinement, and this imprints the A phase on the bulk chamber. If so, it may be possible to seed nonequilibrium phases of superfluid ^{3}He, such as the polar

phase, by cooling through a channel in which the polar phase is stabilized by oriented nanoscale structures [58,60–62].

The quest to understand the nucleation of the B phase from A phase remains open, with implications for cosmology. First order transitions have been proposed in the early universe, such as the electroweak transition [63], and in eternal inflation [64]. These have potential signature signals in future gravitational wave detectors [65–67], the prediction of which relies on nucleation theory. This provides strong motivation to identify the possible intrinsic nucleation mechanisms in superfluid ^{3}He as a laboratory-based simulator for cosmology.

We acknowledge useful input from J. A. Sauls, B. Widom, H. Tye, M. Hindmarsh, and A. J. Leggett. This work at Cornell was supported by the NSF under DMR-1708341, 2002692 (Parpia), PHY-1806357 (Mueller), and in London by the EPSRC under EP/R04533X/1 and STFC under ST/T006749/1. Fabrication of the channel was carried out at the Cornell Nanoscale Science and Technology Facility (CNF) with assistance and advice from technical staff. The CNF is a member of the National Nanotechnology Coordinated Infrastructure (NNCI), which is supported by the National Science Foundation (Grant No. NNCI-1542081).

*Corresponding author.
jmp9@cornell.edu

[1] A. J. Leggett, Rev. Mod. Phys. **47**, 331 (1975).
[2] J. C. Wheatley, Rev. Mod. Phys. **47**, 415 (1975).
[3] D. M. Lee, Rev. Mod. Phys. **69**, 645 (1997).
[4] E. Dobbs, *Helium Three*, International Series of Monographs on Physics (Oxford University Press, New York, 2001).
[5] D. Vollhardt and P. Wolfle, *The Superfluid Phases of Helium 3*, Dover Books on Physics (Dover Publications, New York, 2013).
[6] D. S. Greywall, Phys. Rev. B **33**, 7520 (1986).
[7] R. Rusby, B. Fellmuth, J. Engert, W. Fogle, E. Adams, L. Pitre, and M. Durieux, J. Low Temp. Phys. **149**, 156 (2007).
[8] P. Schiffer, M. T. O'Keefe, M. D. Hildreth, H. Fukuyama, and D. D. Osheroff, Phys. Rev. Lett. **69**, 120 (1992).
[9] D. D. Osheroff and M. C. Cross, Phys. Rev. Lett. **38**, 905 (1977).
[10] J. W. Cahn and J. E. Hilliard, J. Chem. Phys. **28**, 258 (1958).
[11] R. L. Kleinberg, D. N. Paulson, R. A. Webb, and J. C. Wheatley, J. Low Temp. Phys. **17**, 521 (1974).
[12] P. J. Hakonen, M. Krusius, M. M. Salomaa, and J. T. Simola, Phys. Rev. Lett. **54**, 245 (1985).
[13] D. S. Buchanan, G. W. Swift, and J. C. Wheatley, Phys. Rev. Lett. **57**, 341 (1986).
[14] H. Fukuyama, H. Ishimoto, T. Tazaki, and S. Ogawa, Phys. Rev. B **36**, 8921 (1987).
[15] G. W. Swift and D. S. Buchanan, Jpn. J. Appl. Phys. **26**, 1828 (1987).
[16] S. T. P. Boyd and G. W. Swift, Phys. Rev. Lett. **64**, 894 (1990).
[17] C. Bäuerle, Yu. M. Bunkov, S. N. Fisher, H. Godfrin, and G. R. Pickett, Nature (London) **382**, 332 (1996).
[18] V. M. H. Ruutu, V. B. Eltsov, A. J. Gill, T. W. B. Kibble, M. Krusius, Y. G. Makhlin, B. Plaçais, G. E. Volovik, and W. Xu, Nature (London) **382**, 334 (1996).
[19] Yu. M. Bunkov and O. D. Timofeevskaya, Phys. Rev. Lett. **80**, 4927 (1998).
[20] M. Bartkowiak, S. N. Fisher, A. M. Guénault, R. P. Haley, G. R. Pickett, G. N. Plenderleith, and P. Skyba, Phys. Rev. Lett. **85**, 4321 (2000).
[21] See Supplemental Material at http://link.aps.org/supplemental/10.1103/PhysRevLett.126.215301 for supplementary notes and figures, which includes Refs. [6–8,10, 12,14,15,22–33].
[22] J. M. Parpia, Ph.D. thesis, Cornell University, 1979.
[23] J. M. Parpia and J. D. Reppy, Phys. Rev. Lett. **43**, 1332 (1979).
[24] K. Andres and W. Sprenger, edited by M. Krusius and M. Vuorio *Proceedings of LT14*, Vol. 1 (North Holland, 1976), p. 123.
[25] P. G. Debenedetti, *Metastable Liquids Concepts and Principles* (Princeton University Press, Princeton, N.J., 1996), Chap. 2,3, pp. 63–233.
[26] L. Xu, P. Kumar, S. V. Buldyrev, S.-H. Chen, P. H. Poole, F. Sciortino, and H. E. Stanley, Proc. Natl. Acad. Sci. U.S.A. **102**, 16558 (2005).
[27] L. H. Kjäldman, J. Kurkijärvi, and D. Rainer, J. Low Temp. Phys. **33**, 577 (1978).
[28] V. Kotsubo, K. D. Hahn, and J. M. Parpia, Phys. Rev. Lett. **58**, 804 (1987).
[29] A. J. Leggett and S. K. Yip, in Helium Three, *Modern Problems in Condensed Matter Sciences* No. 26, edited by L. P. Pitaevskii and W. P. Halperin (Elsevier, Amsterdam, 1990), 3rd ed., Chap. 8, pp. 523–707.
[30] D. Lotnyk, A. Eyal, N. Zhelev, T. S. Abhilash, E. N. Smith, M. Terilli, J. Wilson, E. Mueller, D. Einzel, J. Saunders, and J. M. Parpia, Nat. Commun. **11**, 4843 (2020).
[31] P. Schienbein and D. Marx, Phys. Rev. E **98**, 022104 (2018).
[32] D. N. Paulson, H. Kojima, and J. C. Wheatley, Phys. Rev. Lett. **32**, 1098 (1974).
[33] N. Zhelev, T. S. Abhilash, R. G. Bennett, E. N. Smith, B. Ilic, J. M. Parpia, L. V. Levitin, X. Rojas, A. Casey, and J. Saunders, Rev. Sci. Instrum. **89**, 073902 (2018).
[34] A. J. Leggett, Phys. Rev. Lett. **54**, 246 (1985).
[35] S. Yip and A. J. Leggett, Phys. Rev. Lett. **57**, 345 (1986).
[36] A. J. Leggett, J. Low Temp. Phys. **126**, 775 (2002).
[37] T. W. B. Kibble, J. Phys. A **9**, 1387 (1976).
[38] W. H. Zurek, Nature (London) **317**, 505 (1985).
[39] D. Ki Hong, J. Low Temp. Phys. **71**, 483 (1988).
[40] S.-H. H. Tye and D. Wohns, Phys. Rev. B **84**, 184518 (2011).
[41] G. E. Volovik, *The Universe in a Helium Droplet* (Oxford University Press, New York, 2002).
[42] P. Schiffer and D. D. Osheroff, Rev. Mod. Phys. **67**, 491 (1995).
[43] Yu. Bunkov, J. Phys. Condens. Matter **25**, 404205 (2013).
[44] G. Barton and M. A. Moore, J. Low Temp. Phys. **21**, 489 (1975).

[45] V. I. Marchenko, Zh. Eksp. Teor. Fiz. **93**, 141 (1987) [Sov. Phys. JETP **66**, 79 (1987)], http://www.jetp.ac.ru/cgi-bin/e/index/r/93/1/p141?a=list.
[46] L. V. Levitin, B. Yager, L. Sumner, B. Cowan, A. J. Casey, J. Saunders, N. Zhelev, R. G. Bennett, and J. M. Parpia, Phys. Rev. Lett. **122**, 085301 (2019).
[47] N. Zhelev, T. S. Abhilash, E. N. Smith, R. G. Bennett, X. Rojas, L. Levitin, J. Saunders, and J. M. Parpia, Nat. Commun. **8**, 15963 (2017).
[48] R. Blaauwgeers, M. Blazkova, M. Človečko, V. B. Eltsov, R. de Graaf, J. Hosio, M. Krusius, D. Schmoranzer, W. Schoepe, L. Skrbek, P. Skyba, R. E. Solntsev, and D. E. Zmeev, J. Low Temp. Phys. **146**, 537 (2007).
[49] L. V. Levitin, R. G. Bennett, A. Casey, B. Cowan, J. Saunders, D. Drung, T. Schurig, and J. M. Parpia, Science **340**, 841 (2013).
[50] A. J. Shook, V. Vadakkumbatt, P. Senarath Yapa, C. Doolin, R. Boyack, P. H. Kim, G. G. Popowich, F. Souris, H. Christani, J. Maciejko, and J. P. Davis, Phys. Rev. Lett. **124**, 015301 (2020).
[51] Y. Tsutsumi, M. Ichioka, and K. Machida, Phys. Rev. B **83**, 094510 (2011).
[52] P. J. Heikkinen, A. Casey, L. V. Levitin, X. Rojas, A. Vorontsov, P. Sharma, N. Zhelev, J. M. Parpia, and J. Saunders, Nat. Commun. **12**, 1574 (2021).
[53] M. M. Salomaa and G. E. Volovik, Phys. Rev. B **37**, 9298 (1988).
[54] I. Yang, S.-H. H. Tye, and B. Shlaer, arXiv:1110.2045.
[55] J. J. Wiman and J. A. Sauls, Phys. Rev. B **92**, 144515 (2015).
[56] S. M. Tholen and J. M. Parpia, Phys. Rev. Lett. **67**, 334 (1991).
[57] S. M. Tholen and J. M. Parpia, Phys. Rev. B **47**, 319 (1993).
[58] J. J. Wiman and J. A. Sauls, J. Low Temp. Phys. **175**, 17 (2014).
[59] L. V. Levitin, R. G. Bennett, E. V. Surovtsev, J. M. Parpia, B. Cowan, A. J. Casey, and J. Saunders, Phys. Rev. Lett. **111**, 235304 (2013).
[60] J. Pollanen, J. I. A. Li, C. A. Collett, W. P. Gannon, W. J. Halperin, and J. A. Sauls, Nat. Phys. **8**, 317 (2012).
[61] V. V. Dmitriev, A. A. Senin, A. A. Soldatov, and A. N. Yudin, Phys. Rev. Lett. **115**, 165304 (2015).
[62] N. Zhelev, M. Reichl, T. S. Abhilash, E. N. Smith, K. X. Nguyen, E. J. Mueller, and J. M. Parpia, Nat. Commun. **7**, 12975 (2016).
[63] A. Katz and M. Perelstein, J. High Energy Phys. 07 (2014) 108.
[64] A. H. Guth, J. Phys. A **40**, 6811 (2007).
[65] P. Amaro-Seoane *et al.*, arXiv:1702.00786.
[66] M. Hindmarsh and M. Hijazi, J. Cosmol. Astropart. Phys. 12 (2019) 062.
[67] C. Caprini, M. Chala, G. C. Dorsch, M. Hindmarsh, S. J. Huber, T. Konstandin, J. Kozaczuk, G. Nardini, J. M. No, K. Rummukainen, P. Schwaller, G. Servant, A. Tranberg, and D. J. Weir, J. Cosmol. Astropart. Phys. 03 (2020) 024.